Positron annihilation lifetime spectroscopy study of polyvinylpyrrolidone-added polyvinylidene fluoride membranes: Investigation of free volume and permeation relationships

Bilge Eren,[1] **Erdal Eren**,[1] **Murat Guney**,[1] **Yan-Ching Jean**,[2] **J. David Van Horn**[2]

[1]Faculty of Science and Arts, Department of Chemistry, Bilecik Seyh Edebali University, 11210, Bilecik, Turkey
[2]Department of Chemistry, University of Missouri-Kansas City, Kansas City, Missouri 64110
Correspondence to: B. Eren (E-mail: bilge.eren@bilecik.edu.tr)

Received 12 September 2019; Revised 30 December 2019; accepted 6 January 2020; published online 20 January 2020
DOI: 10.1002/pol.20190031

ABSTRACT: Polyvinylidene fluoride (PVDF) membranes were prepared via the phase inversion method from casting solutions containing PVDF, dimethylformamide (DMF), and polyvinylpyrrolidone (PVP) as pore former. PVP was used in the casting solution in a range of 0–5 wt % and extracted. The effect on membranes of using PVP in the casting process was analyzed by X-ray diffraction, differential scanning calorimetry, scanning electron microscopy, viscosity, and water permeability techniques. With an increase of PVP from 0 to 5 wt %, the PVDF casting solution viscosities increased from 858 to 1148 cP; the resulting PVDF membrane thickness increased; and the crystallinity of PVDF membranes decreased from 40.0 to 33.3%, which indicates that the addition of PVP inhibits the degree of crystallization in the PVDF membranes. SEM results revealed the shape and size of macropores in the membranes; these macropores changed after PVP addition to the casting solutions. The impact of structural changes on free-volume properties was evaluated using positron annihilation lifetime spectroscopy (PALS) studies. PALS analysis indicated no effect on the average radius (~3.4 Å) of membrane free-volume holes from the addition of PVP to the casting solution. However, the percentage of *o*-Ps pick-off annihilation intensity, I_3, increased from 1.7 to 5.1% with increased PVP content. Further, increasing the PVP content from 0.5 to 5% resulted in an increased final pure water permeability flux. For instance, the 210 min flux for a 14% PVDF + 0.5% PVP membrane was found to be 3.3 times greater than a control membrane having the same PVDF concentration. © 2020 Wiley Periodicals, Inc. J. Polym. Sci. **2020**, *58*, 589–598

KEYWORDS: free volume; microstructure; PVDF membrane; pore former; positron annihilation lifetime spectroscopy

INTRODUCTION Polyvinylidene fluoride (PVDF) can be used for membrane filtration studies thanks to its excellent chemical, mechanical, thermal stability, low surface energy, and low dielectric constant properties.[1] PVDF membranes used for filtration processes are prepared by phase inversion methods and whose structure and performance mainly depend on the composition of casting solution and the coagulation bath.[1,2] Various organic or inorganic additives are used in PVDF membrane fabrication to improve their performance. Organic additives are typically glycerol, ethylene glycol, polyethylene glycol (PEG), and polyvinylpyrrolidone (PVP); examples of inorganic additives include LiCl, $LiClO_4$, or $ZnCl_2$.[1,2]

The presence of a nonsolvent additive in a polymer casting solution alters the thermodynamic and kinetic characteristics in the phase inversion process. Depending on amounts of the nonsolvent additive, two opposite effects may be observed in membrane formation processes. First, the additive may decrease the miscibility between water and the casting solution, which enhances the thermodynamic equilibrium toward the phase inversion. Second, the additive could also make the casting solution highly viscous, causing a kinetic hindrance against phase inversion.[3–6]

PVP is used extensively as a nonsolvent additive in polymer casting solutions for fabricating asymmetric PVDF membranes due to its solubility in water and miscibility with PVDF. The use of PVP, among other additives, in casting solutions, developments in graft polymers, and the wide investigation of techniques that produce asymmetric membranes is an ongoing significant endeavor.[7] It has been reported that PVP/water solubility affects PVDF casting solution phase inversion because the formation of the resulting membrane is largely controlled by thermodynamic or kinetic properties of the mixture at differing conditions.[8,9] To elaborate, the phase separation process is controlled by variation in the thermodynamic property at low PVP concentrations, but there is a threshold content, above which kinetic processes predominate. The threshold values for PVP-added PVDF membranes were found in a content range of 6–9 wt %.[8,9] In these studies, an increase

© 2020 Wiley Periodicals, Inc.

in PVP content in casting solutions reduced the rates of demixing and exhibited increased kinetic hindrance in the higher viscosity solution.

To further demonstrate that solution viscosity results in a hindrance of solution kinetics and delayed demixing, Zhou and Xi showed that a PVP content above 3 wt % in PVDF membrane casting solutions also caused these effects.[10] Wang *et al*. have studied hollow fiber membranes made up of PVDF by changing the amount and molecular weights of PVP (MWs of 10 K, 24 K, 360 K) in casting mixtures. Here, the membranes with lower PVP content exhibited a low water flux and high rejection properties. In contrast, membranes with a high PVDF and low PVP composition showed an excellent mechanical strength. In the presence of low concentrations of low-molecular weight PVP, membrane porosity was higher than when a high-molecular weight PVP was used.[11] In another study, Kong and Li investigated hollow-fiber PVDF membranes cast from mixtures with and without added PVP.[12] The results revealed that the PVP additive has a miniscule effect on the average membrane pore size but enormously increased (two orders of magnitude) the effective membrane porosity; the PVP-added PVDF hollow-fiber membranes possessed extremely large macrovoids and cavities at both the inner and outer skins. It was noticed that the thickness of the sponge-like morphology at the core of the wall fiber in PVP-added membranes was diminished compared to PVDF membranes with no added PVP. This thickness was attributed to the hydrophilic nature of PVP leading to an enhancement of the precipitation rate of PVDF during the casting process. Lang *et al*. found decreases in both the precipitation rate and the instantaneous demixing mechanism of membrane formation as the molecular weight of PVP increases (from MW 58 K to 1.3 M) in PVDF/PVP/NMP casting solutions.[13] Small peaks were observed in the precipitation curves of the doped PVDF solution that contained low-molecular weight PVP. The high-molecular weight PVP posed a restriction in the formation of macropores in the interior surface of the PVDF membranes with an increase in viscosity of the dope. In as-spun PVDF membranes, the pure water permeability (PWP) rises initially and then falls with the increase in PVP molecular weight. Mhlanga *et al*. used contact angle measurements to determine that PVDF membrane hydrophilicity increased with an increase in PVP content from 3 to 10 wt %.[14] Analysis of the same membranes via SEM showed pore size increases with added PVP. Additionally, unsupported PDVF membranes exhibited a decrease in tensile strength with increases in PVP content. Finally, a study from Cha and Yang shows that PVDF membrane structure without PVP is clearly different from that prepared with PVP.[15] Here, the pore structure of hollow fiber membranes with and without PVP was studied by capillary flow porometry techniques and showed that PVP addition led to reduced average pore sizes in the produced membranes.

Polymer filtration membranes include two kinds of nanoscopic-sized pores—"network" and "aggregate" pores.[16] The first of these, network pores, is comprised of the small voids between the aggregated polymer chains; in contrast, the second type, aggregate pores, is larger voids interspersed between regions of polymer aggregates. Positron annihilation lifetime spectroscopy (PALS) can characterize varied nanoscopic membrane pore sizes and be correlated to membrane properties.[17–21] This technique is especially useful for membranes having network pore radii around 0.1 to 0.3 nm and aggregate pore radii ranging from 0.3 to 0.6 nm.[19–21] In comparison to either network or aggregate pore size in membranes, the water molecule is smaller, having a radius of about 0.137 nm.[22] Membrane permeation flux performance may be a function of both network and aggregate pores; and overall membrane free volume is understood to correlate to permeation flux, as flux follows the free-volume trends observed in PALS determinations.[23–25]

Polyamide-based, high-performance permeable membranes for reverse osmosis or nanofiltration are associated with the lower rejection rates,[26–29] and some researchers reported that there is not a direct relation between permeability and rejection properties of the membranes.[30–35] Nanda *et al*. claimed that the presence of molecular size vacancies in nonporous membranes triggers the increased flux and decreased salt rejections observed in fouled membranes.[36] They also proposed that PALS techniques are an apt choice for studying the morphological changes that defines the membrane performance. Peng *et al*. have investigated annealing temperature effects, swelling related to annealing time, the sorption properties, and pervaporation properties of hybrid PVA-GPTMS membranes using PALS.[19] They found that their hybrid membrane separation performance is interrelated with the free-volume characteristics of the membrane, which includes microvoid cavity size and quantity. Ong and Tan have reported the effective separation of a ternary azeotropic mixture of ethyl acetate, ethanol, and water in contact with buckypaper membranes immobilized with a blend of poly(vinyl alcohol) and an ionic liquid, 1-butyl-3-methylimidazolium tetrafluoroborate.[37] They described an increase in permeation flux related to feed temperature in their system, and they noted that this may be anticipated because of free volume size increases with thermal expansion of the membrane, among other factors (increased solute partial pressures and overall energy in the solution).[37] Zhao *et al*. found that the incorporation a hydrophilic additive increases the amount of free volume of a polyamide thin film composite membrane, which allows the flux of both water and salt.[38] The observation of decreased salt rejection is ascribed to both increased hydrophilicity and increased free volume in the prepared membranes.

Based on the aforementioned discussion, separation performance is closely associated with the free-volume features of the membranes, namely cavity sizes and their abundance. Thus, in the present study, we have investigated the relationship between the PVP content as a pore former in PVDF membrane casting solutions and the free-volume characteristics of the resulting PVDF membranes. PVDF membranes derived from PVP-added casting mixtures were prepared using phase inversion methods. The effect of PVP-added mixtures on the resulting membranes' flux performance and bovine serum

albumin (BSA) rejection properties were compared to free-volume measurements using PALS. In addition, effects related to PVP-added content on membranes' crystallization, morphology and rheological properties were also investigated.

EXPERIMENTAL

Materials

PVDF (d = 1.780; mp: 155 °C) was used as received (ABCR, Germany). Dimethylformamide (DMF) and polyvinylpyrrolidone (PVP) (MW 360,000) were used as received (Sigma-Aldrich Co.). The separation performance of the resulting PVDF membranes was characterized using bovine serum albumin (BSA, MW 67,000).

Membrane Preparation

The phase inversion method was employed to prepare the flat sheet PVDF membranes. For all casting solutions, the weight content of PVDF to total casting solution was 14 wt %, and the weight content of PVP to total casting solution was varied from 0 to 5.0 wt %, and each solution was stirred for 10 h at 60°C. The solutions were degassed after the complete dissolution of polymers in an ultrasonic water bath for 2 h. The liquid was uniformly cast onto a glass plate using a casting knife with a gap of 200 μm; the plate was immersed immediately in a coagulation bath (ultrapure water) at room temperature. The resulting sheets were washed and submerged in DI water to remove any residual DMF. The membranes were finally dried at room temperature before testing. Membrane sample designations and compositions are given in Table 1.

Membrane Characterization

The prepared membranes were characterized by the following methods:

1. Casting solution viscosities of PVP-added PVDF mixtures were evaluated using a Brookfield DV-II+ Pro (USA) instrument. Viscosity measurements were conducted at 23 °C using cone/cup geometry with a spindle multiplier constant (SMC) of 128 and between 70 and 105 rpm.

2. Casting dope cloud points were determined by measuring the number of aliquots of distilled water that were added to produce a cloudy mixture.

TABLE 1 Contents of PVDF membrane casting solutions

Membrane	PVDF (wt %)	PVP (wt %)	DMF (wt %)
PVDF-00	14	0.0	86.0
PVDF-10	14	0.5	85.5
PVDF-20	14	1.0	85.0
PVDF-30	14	2.0	84.0
PVDF-40	14	4.0	82.0
PVDF-50	14	5.0	81.0

3. The morphologies of the membranes were observed in cross-sectional views by SEM (Carl Zeiss Sigma VP) after coating with platinum.

4. The membranes' thermal behavior was observed using a Shimadzu DSC-60 differential scanning calorimeter. Thermograms obtained from a temperature program of 25–300 °C at 10 °C/min under a N_2 atmosphere were used to determine membrane melting points and the heats of fusion (ΔH_f).

5. XRD measurements were taken on uncoated membrane samples (Fig. 1) with a PAN Analytical X-ray Systems (XRD Rigaku Miniflex) (Cu Kα radiation, λ = 1.54 Å).

6. All permeation tests were conducted in a custom-made, cross-flow ultrafiltration cell with a 47 mm diameter membrane. Three trials were performed separately to determine mean values and standard deviations. Membrane porosity, pure water flux (PWF), water uptake, and compaction properties were measured as previously described.[39]

7. The PWF was measured by direct measurement of the permeate flow (L/m^{2}h). PWF was measured at different transmembrane pressures (80, 150, 200, 250 and 300 kPa) after a compaction time of 8 h and calculated using:

$$J_w = \frac{Q}{A\,\Delta t} \quad (1)$$

where J_w is the flux (L/m^{2}h), Q is the quantity of permeate collected (L), A is the effective membrane surface area (m^2), and Δt is the sampling time (h). The solute rejection performance of the fabricated membranes was investigated using BSA as a model protein. BSA was dissolved in a phosphate buffer (0.05 M, pH 7.0) and adjusted to a concentration of 500 mg L^{-1} for the entire study. The membrane BSA rejection experiments were carried out at 200 kPa and the final BSA concentrations were determined via spectrophotometry (PG instruments, T80) at 280 nm.[39] The BSA rejection ratio was calculated by the following equation:

$$\mathrm{SR}\,(\%) = \left(1 - \frac{C_p}{C_f}\right) \times 100 \quad (2)$$

where C_p and C_f are the concentrations in permeate and the feed, respectively. After BSA rejection experiments, the membranes were washed with deionized water and immersed in distilled water for 20 min for cleaning.

8. Positron annihilation lifetime measurements were determined using a conventional fast–fast gamma coincidence method at 25 °C. The time resolution of the spectrometer was <350 ps, determined by using a ^{60}Co source in the ^{22}Na energy window settings.[40,41] Samples were dried at ambient conditions for at least 30 min before preparing the PALS sample. Narrow (~5 mm) strips of the membrane (0.5–0.15 mm thickness) were wrapped around a Kapton®-sealed ^{22}Na positron source to a thickness of >1 mm to assure that all positron radiation would be contained within the sample. A source correction for positron interaction with the Kapton® coating is considered for the data analysis. All PAL spectra were

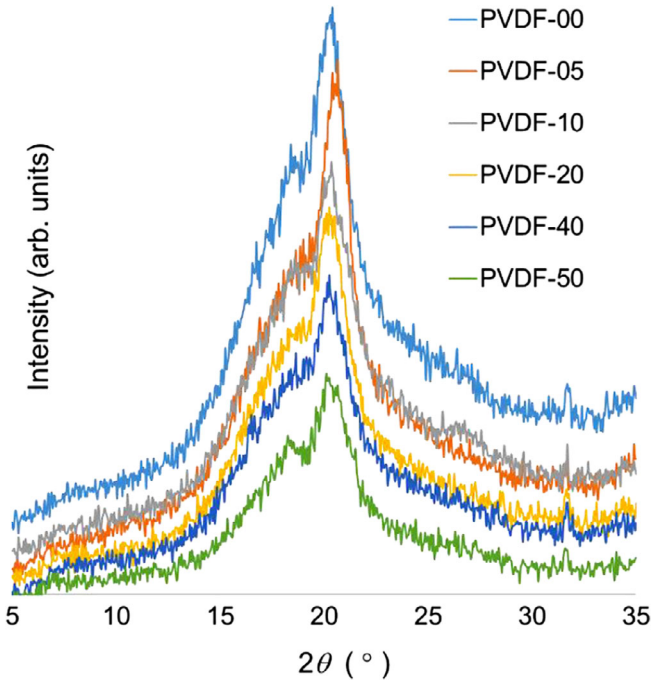

FIGURE 1 XRD spectra for PVDF membranes as a function of PVP content in casting solution. [Color figure can be viewed at wileyonlinelibrary.com]

resolved into three or four components (see discussion) using the PATFIT program.[42] Each PAL spectrum was fitted to three or four exponential lifetime components, which are assigned as follows: the shortest lifetime, $\tau_1 \approx 0.125$ ns, is attributed to *para*-Ps (the singlet Ps state) annihilation; the intermediate lifetime ($\tau_2 \approx 0.4$ ns) is due to bulk positron annihilation, and the component with the longest lifetime ($\tau_3 \approx 1.8$–2.1 ns) and its relative intensity (I_3) is due to pick-off annihilation of *ortho*-Ps. The fourth component ($\tau_4 \approx 50$ ns) is an *ortho*-Ps lifetime associated with large void/pore volumes in samples containing mesoscopic void structure.[21] The observed *o*-Ps pick-off lifetime has been correlated with the size of free volume holes, and the corresponding intensity (I_3) may be correlated with an apparent free volume fraction (ffv) from positron annihilation data.[41] The voids are assumed spherical for the basis of the present analysis, as described before.[43,44] A modified Tao-Eldrup model, a robust semi-empirical equation for free volume calculation, is applied here by fitting measured *o*-Ps lifetimes (τ_3) in a spherical potential well with established sizes of radius, R:

$$\tau_3 = 0.5 \times \left[1 - \frac{R}{R+\Delta R} + \frac{1}{2\pi}\sin\left(\frac{2\pi R}{R+\Delta R}\right)\right]^{-1} \quad (3)$$

where τ_3 and R, are in units of ns and Å, respectively, and ΔR was calibrated to be 1.656 Å.[45,46] This equation is good for most polymeric materials, and for spherical void sizes up to about 1 nm, corresponding to approximately 10 ns *o*-Ps lifetimes. In certain membranes or polymers, the size of voids may vary from angstrom into the submicron range.

Recently, correlation to void volume size has been extended to include the 3γ process from *o*-Ps and modified for hole sizes between 1 and 100 nm, corresponding to observed lifetimes longer than 10 ns.[43,44,47]

RESULTS AND DISCUSSION

Material Characterization

XRD analysis was used to investigate the crystallization of PVDF membranes in this study. XRD patterns of PVDF and PVP-added PVDF membranes are depicted in Figure 1. Characteristic peaks of the α and β crystalline phases of PVDF could not be clearly identified in the spectra due to a broad, intense peak at about $2\theta = 20.4°$. The crystalline form of PVDF typically exhibits a mixture of these α and β crystalline domains.[48] In the membranes produced here, the relative intensity of the broad peak decreases with the addition and increasing percentage of PVP as a component of the casting solution. As proposed before, the addition of PVP reorganizes PVDF chains in the casting solution and thus reduces the resulting crystallinity of PVDF[15] while not changing the expected PVDF crystalline phases. The relative intensity of the broad XRD peak decreased with PVP increase up to 3 wt %. This change may be due to the influence of PVP on the recrystallization kinetics of PVDF chains to promote localized amorphous regions, leading to a decrease in crystallinity in the membrane. A further increase of added PVP, to 5 wt%, increased the relative intensity of the broad peak, which could be attributed to the phase separation of PVP from the PVDF matrix with each phase either rich in PVDF or in PVP, respectively.

TABLE 2 The properties of the PVDF membranes prepared in the present study

Sample	PVP (%)[a]	Thickness (μm)[b]	Viscosity (cP)[b]	T_m (°C)	Crystallinity (%)[c]	Intensity (%)[b]
PVDF-00	0.0	50	858	161.7	40.0	2.194
PVDF-05	0.5	60	861	160.6	38.8	1.650
PVDF-10	1.0	70	869	160.4	38.7	1.439
PVDF-20	2.0	110	880	160.2	37.0	1.070
PVDF-40	4.0	180	1036	160.1	37.2	1.699
PVDF-50	5.0	170	1148	160.2	33.3	2.155

[a] The weight percentage (wt %) added PVP in casting solution.
[b] From the main X-ray diffraction peak at $2\theta = 20.4°$.
[c] Obtained from DSC.

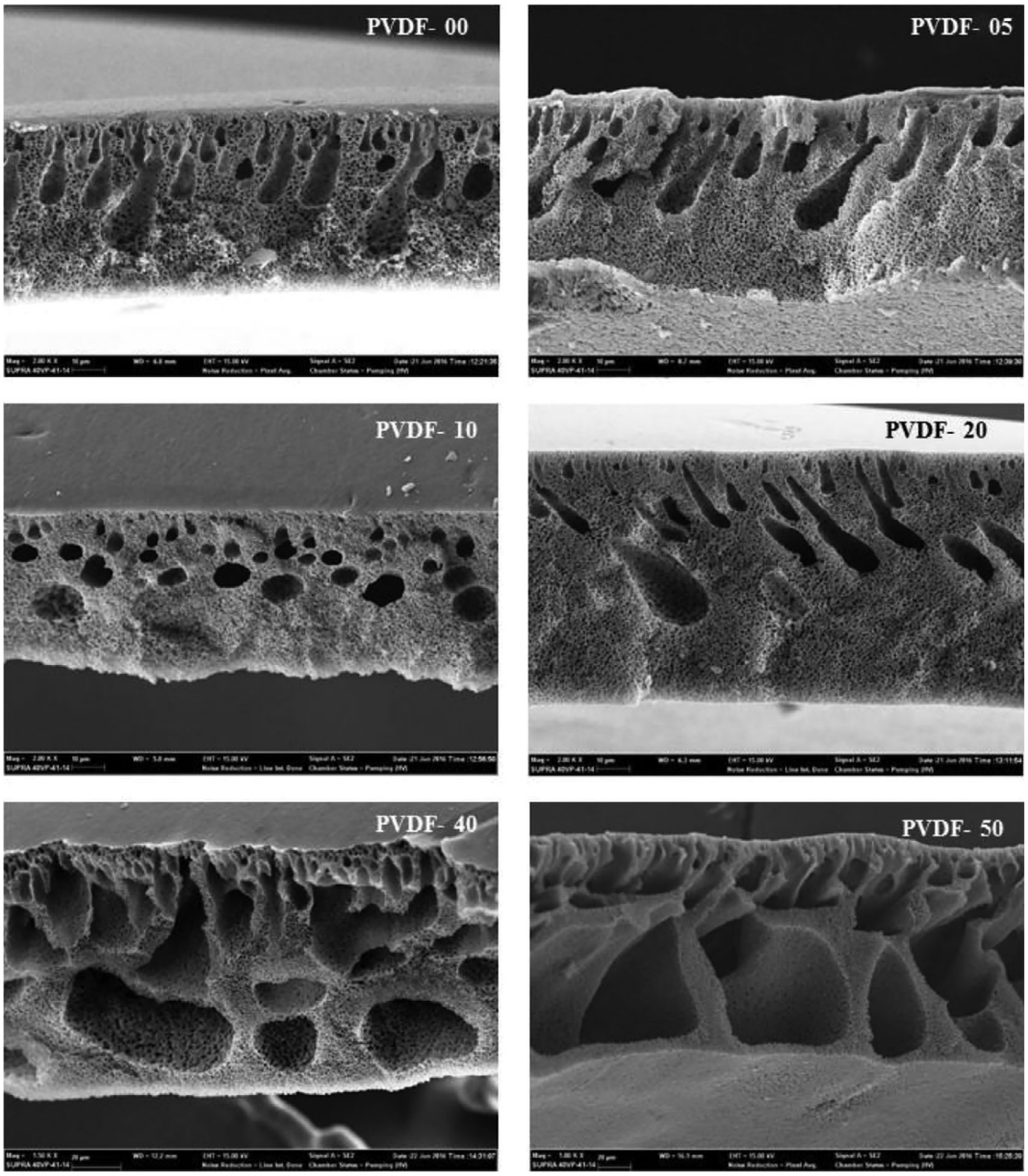

FIGURE 2 Morphological changes in PVDF membranes as a function of PVP content in casting mixtures.

Differential scanning calorimetry (DSC) is typically the most common and useful technique to determine the phase change behavior in polymeric materials. DSC analysis was done here to compare the degree of crystallinity of pristine PVDF and PVP-added PVDF membranes. Here, PVDF membrane melting temperature (T_m) decreased with the addition of PVP (Table 2). This result points to PVP affecting the PVDF polymer casting solution, producing changes in the resulting crystalline structures of PVDF during the precipitation process. Similar results have been obtained in different polymer systems when using PVP or other additives.[13,15,49–52] These changes may be attributed to the alteration in thermodynamic properties of the phase inversion with the introduction of PVP as pore former. During crystallization of PVDF in the presence of PVP, the two polymers separate into a PVDF- or PVP-rich phases. The phase separation process is impeded as the PVP content is increased in the casting polymer solution. This may be attributed to increased hydrogen bonding between hydrogen atoms of PVDF and carbonyl groups of PVP.[39] This slower phase separation suppresses the crystallization of PVDF polymer chains.

To further elaborate, casting solution additives can produce two opposite effects that depend on their concentrations. The additive may lead to a reduction of the miscibility of the casting solution with water; this incompatibility of components in the mixture augments the driving force in the thermodynamic equilibrium to favor the phase inversion process. In contrast,

TABLE 3 Change in *ortho*-Ps lifetimes [τ_3] and intensity [I_3] for modified PVDF membranes as a function of PVP added to PVDF casting solution, with associated PALS variance of fit (VOF), and free volume (fv) size estimates including calculated radius (R), the calculated fv and calculated fractional free volume (ffv). Also, observation of a long lifetime component [τ_4] and associated intensity [I_4] for modified PVDF membranes. An uncalibrated estimate for the size of the larger voids in the material, derived from the τ_4 value, is ~16 Å (see discussion)

Sample	PVP (%)	τ_3 (ns)	I_3 (%)	R (Å)	fv (Å3)	ffv (%)	τ_4 (ns)	I_4 (%)	VOF
PVDF-00	0.0	2.568 ± 0.053	1.87 ± 0.05	3.34 ± 0.03	156 ± 4	0.53 ± 0.03	54 ± 2	0.57 ± 0.05	1.06
PVDF-05	0.5	2.470 ± 0.040	2.48 ± 0.06	3.27 ± 0.02	146 ± 3	0.65 ± 0.03	59 ± 2	0.44 ± 0.05	1.06
PVDF-10	1.0	2.422 ± 0.042	2.36 ± 0.07	3.23 ± 0.03	141 ± 3	0.60 ± 0.03	60 ± 5	0.19 ± 0.05	1.05
PVDF-20	2.0	2.449 ± 0.047	2.21 ± 0.07	3.25 ± 0.03	144 ± 4	0.57 ± 0.03	53 ± 6	0.13 ± 0.05	1.06
PVDF-40	4.0	2.325 ± 0.022	5.20 ± 0.07	3.15 ± 0.01	132 ± 2	1.22 ± 0.03	53 ± 5	0.19 ± 0.05	1.07
PVDF-50	5.0	2.348 ± 0.025	4.14 ± 0.06	3.17 ± 0.02	133 ± 2	0.99 ± 0.03	48 ± 5	0.19 ± 0.05	1.05

the additive in the casting solution may lead to an increase in viscosity such that it creates a kinetic inhibition of the phase inversion.[53,54] The viscosity of the PVDF casting solution affects the membrane morphology by changes in the thermodynamic and kinetic processes in phase inversions during the casting process. Viscosities of the PVDF and PVP-added PVDF casting solutions measured at 25°C are given Table 2. Note that the PVDF solution without PVP has a viscosity of 858 cP. The viscosity values of the casting solution increased from 861 to 1148 cP with the increasing amount of PVP over the range of 0.5–5 wt %. This result is attributed to a decrease of solvent (DMF) in the casting solution due to the dissolution of the added PVP. For this reason, the casting polymer solution becomes thermodynamically less stable, resulting in a demixing rate enhancement and rapid precipitation of the polymer. In this case, the crystallization could be inhibited with simultaneous and rapid phase demixing before the crystalline phase formation occurs. DSC studies indicated that crystallization is reduced at the higher concentration of PVP. This suppression is beneficial for the performance of the membranes, namely the reduced crystallinity leads to a decreased chain orientation in the polymer molecules, further reducing chain packing and increasing the mobility of the polymer in the amorphous regions.[55–57] Therefore, the free volume of the amorphous region is expected to increase with the added PVP

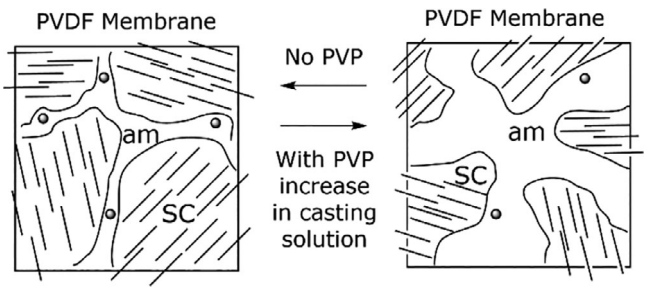

FIGURE 3 Sketch of the nanostructural components in PVDF membranes showing the increase in amorphous (am) versus semicrystalline (SC) regions. The dots represent a notion of the "τ_4" feature in the PALS data. See discussion. Caution! Not to scale; not representative of quantitative changes.

due to the reduced crystallinity. Although each membrane was prepared with the same casting knife (200 μm gap), the actual resulting thickness of membranes increased with increasing amounts of PVP in the casting solution. This is directly related to the formation of large macropores in the membranes during their formation, and is seen in the SEM data (Fig. 2). To account for this, the water inflow-to-DMF outflow ratio increases with addition of PVP and is related to the increased viscosity of the casting solution. In this scenario, the highly viscous nature of casting solution caused the DMF outflow to slow from the casting solution. This slow rate of DMF outflow allows the early stage development of membrane skin, a rapid phase-inversion process, and results in less membrane shrinkage; Liu et al. have extensively compared and described the processes surrounding PVDF membrane preparation.[1]

The performance of polymeric membranes regarding water flux can be correlated with membrane free volume (fv) and fv distribution.[58–63] Positron techniques are widely used for the comparison of material properties as a function of fv in a wide variety of polymeric materials, including membranes.[64,65] In this study, positron lifetime spectra of membrane samples were taken as a function of the content of PVP added to PVDF casting solutions. PALS data were ultimately evaluated using four lifetime components, τ_i, and intensities, I_i. Subscripts i = 1 to 4 are attributed to (a) singlet-state positronium annihilation (*para*-positronium, *p*-Ps), (b) free positron annihilation, (c) *ortho*-positronium (*o*-Ps) annihilation, and (d) a long lifetime annihilation component (also expected to be *o*-Ps), respectively. The *o*-Ps lifetime, τ_3, assigned to pick-off annihilation processes within material voids is longer in larger free-volume voids, and has been correlated to the free volume size. The *o*-Ps intensity, I_3, is related to the concentration of the voids or defects (i.e., the amount) in a polymeric or material sample.[66,67]

Ortho-Ps pick-off lifetimes, intensities, and the calculated free-volume properties of the PVDF membrane and PVP-added PVDF membranes are given in Table 3. The value of *o*-Ps intensity, I_3, and the apparent ffv for all the PVP-added PVDF membranes is higher than that of the original PVDF and fluctuates in linearity. I_3 reaches its highest value when 4 wt %

PVP was added and then decreased slightly for the 5 wt % PVP-added membrane. Here, the crystallinity (i.e., the physical structure) rather than the chemical environment (only C, H, and F atoms in PVDF) predominantly influences the relative intensities of *o*-Ps formed (I_3). In the membranes studied here, τ_3 decreases slightly with increasing PVP content, resulting in a similar trend for the calculated radius; the smallest free-volume cavities have average radii ranging from 3.34 to 3.15 Å.

Since the PVP-added PVDF membranes revealed a free-volume cavity radii near 3.2 Å, water is expected to easily permeate through the material.[11,68] Increased ffv (calculated as %) was observed in the PVP-added PVDF membranes compared to the PVDF-only membrane. The increased ffv of the PVP-added PVDF membranes is mainly attributed to decreased crystallinity in the membrane (Table 2 and Fig. 3); this result from the larger number of defects (free-volume holes) in amorphous regions of polymer chains. The more ordered periodic structure of semicrystalline domains possesses a smaller ffv as the inter-chain distances are, on average, closer, thus reducing the number of fv holes. The ffv observations are corroborated by the XRD and DSC studies that also point to PVP addition changing the PVDF crystallization behavior from the doped casting solutions. The crystallinity of PVDF membranes determined from XRD spectra decreased from 40.0 to 33.3%, thus the addition of PVP in the casting solution ultimately reduces the degree of crystallization in PVDF membrane. Consequently, the decrease of crystallinity also indicates that amorphous PVDF and PVP are miscible. Table 2 also lists the small decrease of melting point with PVP addition. This type of melting point decrease may be understood as the reduction in the formation of crystalline domains and concomitant increase of amorphous segments when PVP is a component in the casting solution.

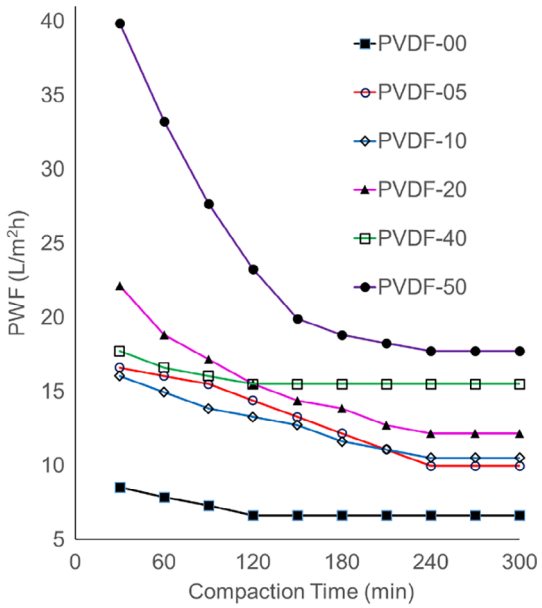

FIGURE 4 Effect of compaction on PWF of PVDF membranes [Color figure can be viewed at wileyonlinelibrary.com]

TABLE 4 Comparison of PWF and BSA rejection performance (SR) for modified PVDF membranes

Sample	PVP (%)	PWF (L/m^{2}h)	SR (%)
PVDF-00	0.0	7.3 ± 0.1	61.5
PVDF-05	0.5	22.1 ± 0.1	61.6
PVDF-10	1.0	11.6 ± 0.2	86.4
PVDF-20	2.0	11.1 ± 0.1	78.5
PVDF-40	4.0	13.8 ± 0.2	77.8
PVDF-50	5.0	18.8 ± 0.2	76.5

Another feature of the PALS data is the observation of a fourth lifetime component (τ_4), attributed to *o*-Ps annihilation in larger voids in the membranes. When spectra were analyzed with a constraint of only three lifetimes, this invariably led to poor fitting of the lifetime spectra and large calculated errors and variance of fit for the data. Thus, all spectra were deconvoluted with an included fourth lifetime (see Table 3). The estimated void size associated with this lifetime is 16 Å,[21,44] and it appears that the concentration of this larger void decreases as PVP is added to the casting solution, down to 1%, after which it remains constant. In some cases, *o*-Ps annihilation intensity (I_3 or I_4) cannot be directly correlated with the void concentration since annihilation intensity is a function of Ps formation probability.[44] The observation of longer lifetimes in PALS will benefit from further study focused on the larger void structures[64,65,69,70] but corresponds here with the morphological changes observed, as PVP is displacing DMF in affecting the final membrane characteristics (compare to the SEM results below).

Figure 2 shows SEM images of PVDF membranes' cross section prepared by increasing the PVP content. The membranes prepared from the polymer casting solution devoid of PVP showed an asymmetric structure variance, featuring a dense top layer and a porous sublayer. The sublayer consists of finger-like cavities in addition to irregular macrovoids. This morphology indicates skin layer formation due to a slow exchange rate between DMF and water at initial stage in the phase inversion processes. The cross-sectional SEM images also revealed an increase in macrovoid sizes with increased PVP concentration. In addition, the dimensions of finger-like cavities significantly diminished, and the macrovoids became larger and predominated the structure.

This observed change in the membrane morphology due to PVP can be accounted for as follows. Because of a high exchange rate between DMF and water, the generation of finger-like pores in the sublayer of PVDF membranes may be attributed to an instantaneous demixing process as was observed previously.[71–74] Further, the presence of PVP-added PVDF casting solution affects the membrane morphology as follows: (a) the water/DMF exchange during phase inversion is severely affected by PVP in the highly viscous casting solution; (b) the hydrophilicity of PVP affects the phase separation

TABLE 5 A performance comparison of different PVDF membranes reported in the literature to those in the present study

Membrane	PWF (L m^{-2} h)	Rejection (%)	References
6% PVP' bore fluid containing 30% EtOH, hollow fiber	8.50 (20 mbar)		8
PVDF:TPU (80:20), 1% PVP, hollow fiber	55.41 (0.1 MPa)		9
Ar gap with 15 cm, hollow fiber	81.9	64 (Dextran)	10
PVP (K 360) added, air gap with 15 cm, hollow fiber	6.7	32.2 (Dextran)	10
PVDF, flat sheet	9.25		50
PVDF modified with 1 wt % HEMA, BPh, 5 min UV, flat sheet	124		77
PVDF modified with 1 wt % AA, BPh, 5 min UV, flat sheet	231		77
PVDF dope-containing 2% LiCl, flat sheet	86.8	84 (Dextran)	78
15% PVDF, 10% PVP, 2% water, flat sheet	116		79
18% PVDF, 2% p(MMA-r-POEM), flat sheet	48.23	20 (BSA)	80
19% PVDF, 2% Al2O3, flat sheet	74.3	96.5	81
Chitosan-modified PVDF, flat sheet	972 (1.5 bar)		82
PVDF-*g*-PVP, 1 min UV, flat sheet	630.8 (42 kPa)		83
PVDF-*g*-PVP, 10 min UV, flat sheet	135.4 (42 kPa)		83
PVDF-*g*-PEGMA, flat sheet	226.1 (1 bar)		84
PVDF-*g*-PEGMA, flat sheet	60–80 (1 bar)		85
PVDF-*co*-HFP/DMF, flat sheet	15.6		86
PVDF/DMAC/TCP, flat sheet	19.1		87
PVDF	7.31 (1 bar)		This study
PVDF dope-containing 0.5 wt % PVP	22.14 (1 bar)		This study
PVDF dope containing 5.0 wt% PVP	18.8 (1 bar)	76.5	This study

kinetics and thereby the thickness of the topmost membrane layer.[71–74] Comparison of the images PVDF-00, PVDF-10, PVDF-20 and PVDF-30 with PVDF-40 and PVDF-50 show that the macropore sizes increased in the middle portion of membranes. The membranes including PVP content higher than 1 wt % in the casting solution (Fig. 2) exhibited the most significant changes in sublayer and skin layer morphologies. With PVP content in the casting solutions greater than 1 wt %, the PVDF and PVP interactions increase with an attendant increase in viscosity (Table 2). This overcomes the driving force for the phase separation and consequently forms membranes with a dense top layer having low porosity.

Membrane Performance Study

PWF is highly dependent on top and middle portions of membranes used in water purification applications.[75–79] A flux increase in a membrane may be explained by an enhanced phase separation by a pore-former.[75] At a low pore-former content, the high demixing rate at the components' interfaces causes the formation of spaces between collapsed polymer aggregates. At a high pore former content, the rate of phase separation is suppressed by increased mixture viscosity. Thus, a low porosity top layer that is dense and relatively thick is developed[76]; this top layer restricts the water diffusion into the membrane structure.[77] Also, the presence of large macrovoids causes substantial compaction and high flux resistance.[78,79] As noted above, SEM results revealed that PVP-added casting solutions produce an increase in the size of macrovoids in the membrane. The values of PWF for all the PVP-added PVDF membranes are greater than those of a PVDF membrane itself and fluctuate in linearity (Fig. 4 and Table 4). This shows that water could pass through polymer-free void gaps or pores. As given in Table 4, the PWF values increased with PVP content, which was consistent with the ffv observed in the positron studies. The formed nanoscale cavities between the polymer chains of membrane, acting as new water channels, provide more free volume, resulting in the increase of the water flux. Finally, the PVP-added PVDF membranes were characterized by estimating rejection and flux during permeation experiments with BSA solution as feed.[39] It is evident that rejection of BSA increases from 61.5 to 86.4% with increase in PVP content in the casting solution over the initial steps from 0 to 0.5 to 1.0 wt %. The further increase in PVP content in casting solutions from 1.0 to 5.0 wt % for PVDF membrane slightly lowers the rejection of BSA from 86.4 to 76.5%. The decrease in BSA rejection is an indication that the average pore size of the skin layer becomes larger in the subsequently prepared membranes.

Comparison of Performance with Previously Reported PVDF Membranes

A comparison of rejection and PWF values of PVDF membranes developed in this investigation and representative

PVDF membranes from the literature is given in Table 5.[8–10,52,77–87] Although direct comparison of the membranes used with other reported membranes is difficult due to the varying experimental conditions employed in those studies, the rejection and PWF values of the present PVDF membranes observed in the present study is generally lower but comparable with others' results.

CONCLUSIONS

In this study, DSC and XRD methods showed that the introduction of PVP into PVDF casting solutions altered membrane PVDF crystallization behavior. The addition of PVP in the casting solutions from 0 to 5 wt % compared to the pristine PVDF membrane shows the development of large macropores in the membranes, as observed in the SEM images; the membrane becomes thicker (total thickness, 170 μm) and more porous. The increased membrane thickness (with increasing PVP) can be ascribed to the formation of very large macropores in the membranes from an enhancement of the water inflow to DMF outflow ratio due to the increased viscosity of the solution prepared for casting. In the PVDF membrane studied here, the addition of a small amount of PVP to the casting solution (0.5, 1.0 wt %) initially results in final membranes that have increased PWF and BSA rejection. Further addition of PVP to casting solutions leads to slightly lower values of PWF and BSA rejection in the finally prepared membranes. The *o*-Ps annihilation lifetime associated with polymer free volume (τ_3) was stable with the increase in the content of PVP. However, the *o*-Ps annihilation intensity, I_3, increased with the PVP content. After reaching the maximum value of 5.1% in the sample having 4 wt % of PVP, the I_3 value *decreased* with the further increase in PVP content. The fraction of free volume of the PVP-added blends is larger than pristine PVDF, but the trend fluctuates a small amount; this reflects the increase in the amount of free-volume voids in the membranes from casting solutions containing PVP. The amount of *o*-Ps formed (reflected as I_3 values) may be relatively related to the membranes' amount of amorphous region, a physical characteristic (Fig. 3), because the polymer chemical makeup and connectivity remains the same (only C, H, and F atoms in PVDF molecules). The interactions of casting solution components and differential phase inversion kinetics lead to the observed changes in membrane morphology. As the constitution of PVDF casting solution is altered with PVP addition, the solution viscosity increases because of enhanced interactions between PVP and DMF. Finally, DMF-water miscibility, combined with PVDF-PVP affinity affect solution demixing rates, thus influencing the resulting structure of the membrane.

ACKNOWLEDGMENTS

The authors thank Bilecik Seyh Edebali University Department of Scientific Research Project Unit for supporting this study as a part of the project 2013-02.BİL.04-03. The authors thank James Murowchick (UMKC Geosciences) and Xiaodong Yan (UMKC Chemistry) for assistance with X-ray diffraction measurements and thank Jon Gage and Sai Siva Kumar P. for reviewing a draft manuscript. The isotopes used were supplied by the U. S. Department of Energy Office of Science by the Isotope Program in the Office of Nuclear Physics.

REFERENCES AND NOTES

1 F. Liu, N. A. Hashim, Y. Liu, M. R. M. Abed, K. Li, *J. Membr. Sci.* **2011**, *375*, 1.

2 M. L. Yeow, Y. T. Liu, K. Li, *J. Appl. Polym. Sci.* **2003**, *90*, 2150.

3 H. J. Kim, R. K. Tyagi, A. E. Fouda, K. Ionasson, *J. Appl. Polym. Sci.* **1996**, *62*, 621.

4 G. R. Guillen, Y. Pan, M. Li, E. M. V. Hoek, *Ind. Eng. Chem. Res.* **2011**, *50*, 3798.

5 J. Chen, J. Li, X. Zhan, X. Han, C. Chen, *Front. Chem. Eng. China* **2010**, *4*, 300.

6 K.-W. Lee, B.-K. Seo, S.-T. Nam, M.-J. Han, *Desalination* **2003**, *159*, 289.

7 H. B. Park, J. Kamcev, L. M. Robeson, M. Elimelech, B. D. Freeman, *Science* **2017**, *356*, eaab0530.

8 S. Simone, A. Figoli, A. Criscuoli, M. C. Carnevale, A. Rosselli, E. Drioli, *J. Membr. Sci.* **2010**, *364*, 219.

9 S. Simone, C. Conidi, C. Ursino, A. Cassano, A. Figoli, *Membranes* **2016**, *6*, 9.

10 Y. Zhou, D.-L. Xi, *Desalination* **2008**, *223*, 438.

11 D. Wang, K. Li, W. K. Teo, *J. Membr. Sci.* **1999**, *163*, 211.

12 J. Kong, K. Li, *J. Appl. Polym. Sci.* **2001**, *81*, 1643.

13 W.-Z. Lang, Y.-J. Guo, L.-F. Chu, *Polym. Adv. Technol.* **2011**, *22*, 1720.

14 S. D. Mhlanga, T. G. Tshabalala, E. N. Nxumalo, B. B. Mamba, *IOP Conf. Ser.: Mater. Sci. Eng.* **2014**, *64*, 012036.

15 B. J. Cha, J. M. Yang, *Macromol. Res.* **2006**, *14*, 596.

16 T. Matsuura, S. Sourirajan, Materials science of reverse-osmosis-ultrafiltration membranes. In *Reverse Osmosis and Ultrafiltration*; S. Sourirajan, T. Matsuura, Eds.; American Chemical Society: Washington, D.C., **1985**, p. 1.

17 J. Zhao, Y. Zhu, G. He, R. Xing, F. Pan, Z. Jiang, P. Zhang, X. Cao, B. Wang, *ACS Appl. Mater. Inter.* **2016**, *8*, 2097.

18 F. Peng, L. Lu, H. Sun, Y. Wang, H. Wu, Z. Jiang, *J. Membr. Sci.* **2006**, *275*, 97.

19 F. Peng, L. Lu, H. Sun, Z. Jiang, *J. Membr. Sci.* **2006**, *281*, 600.

20 F. Peng, L. Lu, H. Sun, Y. Wang, J. Liu, Z. Jiang, *Chem. Mater.* **2005**, *17*, 6790.

21 M. B. Larsen, J. D. Van Horn, F. Wu, M. A. Hillmyer, *Macromolecules* **2017**, *50*, 4363.

22 G. Portella, B. L. de Groot, *Biophys. J.* **2009**, *96*, 925.

23 K. Cao, Z. Jiang, J. Zhao, C. Zhao, C. Gao, F. Pan, B. Wang, X. Cao, J. Yang, *J. Membr. Sci.* **2014**, *469*, 272.

24 J. Wang, Y. Mo, S. Mahendra, E. M. V. Hoek, *J. Membr. Sci.* **2014**, *452*, 415.

25 K. Wang, X. Lin, G. Jiang, J. Z. Liu, L. Jiang, C. M. Doherty, A. J. Hill, T. Xu, H. Wang, *J. Membr. Sci.* **2014**, *471*, 27.

26 H. You, X. Li, Y. Yang, B. Wang, Z. Li, X. Wang, M. Zhu, B. S. Hsiao, *Sep. Purif. Technol.* **2013**, *108*, 143.

27 M. Fathizadeh, A. Aroujalian, A. Raisi, *J. Membr. Sci.* **2011**, *375*, 88.

28 G. M. Geise, H. B. Park, A. C. Sagle, B. D. Freeman, J. E. McGrath, *J. Membr. Sci.* **2011**, *369*, 130.

29 Z. Yang, H. Guo, C. Y. Tang, *J. Membr. Sci.* **2019**, *590*, 117297.

30 K. Yoon, B. S. Hsiao, B. Chu, *J. Membr. Sci.* **2009**, *326*, 484.

31 H. Deng, Y. Xu, Q. Chen, X. Wei, B. Zhu, *J. Membr. Sci.* **2011**, *366*, 363.

32 C. Kong, M. Kanezashi, T. Yamomoto, T. Shintani, T. Tsuru, *J. Membr. Sci.* **2010**, *362*, 76.

33 J.-H. Choi, J. Jegal, W.-N. Kim, *J. Membr. Sci.* **2006**, *284*, 406.

34 Y.-C. Chiang, Y.-Z. Hsub, R.-C. Ruaan, C.-J. Chuang, K.-L. Tung, *J. Membr. Sci.* **2009**, *326*, 19.

35 C. H. Cho, K. Y. Oh, S. K. Kim, J. G. Yeo, P. Sharma, *J. Membr. Sci.* **2011**, *371*, 226.

36 D. Nanda, K.-L. Tung, W.-S. Hung, C.-H. Lo, Y.-C. Jean, K.-R. Lee, C.-C. Hu, J.-Y. Lai, *J. Membr. Sci.* **2011**, *382*, 124.

37 Y. T. Ong, S. H. Tan, *Chem. Eng. Res. Des.* **2016**, *109*, 116.

38 L. Zhao, P. C.-Y. Chang, W. S. W. Ho, *Desalination* **2013**, *308*, 225.

39 E. Eren, A. Sarihan, B. Eren, H. Gumus, F. Ozdemir Kocak, *J. Membr. Sci.* **2015**, *475*, 1.

40 H. M. Chen, J. D. Van Horn, Y. C. Jean, *Defect Diffus. Forum* **2012**, *331*, 275.

41 Y. Wang, H. Nakanishi, Y. C. Jean, T. C. Sandreczki, *J. Polym. Sci. B* **1990**, *28*, 1431.

42 P. Kirkegaard, M. Eldrup, O. E. Mogensen, N. J. Pedersen, *Comput. Phys. Commun.* **1981**, *23*, 307.

43 Z. Xia, M. Trexler, F. Wu, Y. C. Jean, J. D. Van Horn, *Phys. Rev. E* **2014**, *89*, 022603.

44 K. Wada, T. Hyodo, *J. Phys. Conf. Ser.* **2013**, *443*, 012003.

45 S. J. Tao, *J. Chem. Phys.* **1972**, *56*, 5499.

46 Y. C. Jean, *Microchem. J.* **1990**, *42*, 72.

47 K. Ito, H. Nakanishi, Y. Ujihira, *J. Phys. Chem. B* **1999**, *103*, 4555.

48 W. Ma, H. Yuan, X. Wang, *Membranes* **2014**, *4*, 243.

49 S. Rajabzadeh, C. Liang, Y. Ohmukai, T. Maruyama, H. Matsuyama, *J. Membrane Sci.* **2012**, *423–424*, 189.

50 D. R. Dillon, K. K. Tenneti, C. Y. Li, F. K. Ko, I. Sics, B. S. Hsiao, *Polymer* **2006**, *47*, 1678.

51 E. Freirea, O. Bianchib, J. N. Martins, E. E. C. Monteirod, M. Madalena, C. Forte, *J. Non Cryst. Solids* **2012**, *358*, 2674.

52 J.-H. Cao, B.-K. Zhu, Y.-Y. Xu, *J. Membr. Sci.* **2006**, *281*, 446.

53 P.-Y. Zhang, H. Yang, Z. Xu, *Ind. Eng. Chem. Res.* **2012**, *51*, 4388.

54 B. Chakrabarty, A. K. Ghoshal, M. K. Purkait, *J. Membr. Sci.* **2008**, *309*, 209.

55 E.-A. McGonigle, J. J. Liggat, R. A. Pethrick, S. D. Jenkins, J. H. Daly, D. Hayward, *Polymer* **2001**, *42*, 2413.

56 Y. Zhou, D.-L. Xi, *Iran. Polym. J.* **2007**, *16*, 241.

57 Q. An, J.-T. Chen, M. De Guzman, W.-S. Hung, K.-R. Lee, J.-Y. Lai, *Langmuir* **2011**, *27*, 11062.

58 M. Hedenqvist, A. Angelstok, L. Edsberg, P. T. Larsson, U. W. Gedde, *Polymer* **1996**, *37*, 2887.

59 S. Claes, P. Vandezande, S. Mullens, R. Leysen, K. De Sitter, A. Andersson, F. H. J. Maurer, H. Van den Rul, R. Peeters, M. K. Van Bael, *J. Membr. Sci.* **2010**, *351*, 160.

60 E. J. Flynn, D. Keane, J. D. Holmes, M. A. Morris, *J. Colloid. Interf. Sci.* **2012**, *370*, 176.

61 T. Suzuki, R. Tanaka, M. Tahara, Y. Isamu, M. Niinae, L. Lin, J. Wang, J. Luh, O. Coronell, *Water Res.* **2016**, *100*, 326.

62 S. G. Chaudhri, B. H. Rajai, P. S. Singh, *Desalination* **2015**, *367*, 272.

63 Y. Li, T. Verbiest, I. Vankelecom, *J. Membr. Sci.* **2013**, *428*, 63.

64 Y. C. Jean, J. D. Van Horn, W.-S. Hung, K.-R. Lee, *Macromolecules* **2013**, *46*, 7133.

65 S. K. Sharma, P. K. Pujari, *Prog. Polym. Sci.* **2017**, *75*, 31.

66 W. Xie, H. Ju, G. M. Geise, B. D. Freeman, J. I. Mardel, A. J. Hill, J. E. McGrath, *Macromolecules* **2011**, *44*, 4428.

67 J. C. Jansen, M. Macchione, E. Tocci, L. De Lorenzo, Y. P. Yampolskii, O. Sanfirova, V. P. Shantarovich, M. Heuchel, D. Hofmann, E. Drioli, *Macromolecules* **2009**, *42*, 7589.

68 L. Li, S. Y. Zhang, Y. H. Chen, M. J. Liu, Y. F. Ding, X. W. Luo, Z. Pu, W. F. Zhou, S. Li, *Chem. Mater.* **2005**, *17*, 839.

69 M. Sadrzadeh, S. Bhattacharjee, *J. Membr. Sci.* **2013**, *441*, 31.

70 S. H. Yoo, J. H. Kim, J. Y. Jho, J. Won, Y. S. Kang, *J. Membr. Sci.* **2004**, *236*, 203.

71 J. S. Kang, Y. M. Lee, *J. Appl. Polym. Sci.* **2002**, *85*, 57.

72 I. M. Wienk, R. M. Boom, M. A. M. Beerlage, A. M. W. Bulte, C. A. Smolders, H. Strathmann, *J. Membr. Sci.* **1996**, *113*, 361.

73 M.-J. Han, S.-T. Nam, *J. Membr. Sci.* **2002**, *202*, 55.

74 C. Ding, J. Yin, B. Deng, *Chem. Proc. Eng.* **2014**, *1*, 1.

75 X. Ding, Z. Liu, M. Hua, T. Kang, X. Li, Y. Zhang, *J. Appl. Polym. Sci.* **2016**, *133*, 43941.

76 M. T. M. Pendergast, J. M. Nygaard, A. K. Ghosh, E. M. V. Hoek, *Desalination* **2010**, *261*, 255.

77 A. Rahimpour, S. S. Madaeni, S. Zereshki, Y. Mansourpanah, *Appl. Surf. Sci.* **2009**, *255*, 7455.

78 D. Wang, K. Li, W. K. Teo, *J. Membr. Sci.* **2000**, *178*, 13.

79 M. L. Yeow, Y. T. Liu, K. Li, *J. Appl. Polym. Sci.* **2004**, *92*, 1782.

80 J. F. Hester, A. M. Mayes, *J. Membr. Sci.* **2002**, *202*, 119.

81 L. Yan, Y. S. Li, C. B. Xiang, *Polymer* **2005**, *46*, 7701.

82 S. Boributh, A. Chanachai, R. Jiraratananon, *J. Membr. Sci.* **2009**, *342*, 97.

83 M. Zhang, Q. T. Nguyen, Z. Ping, *J. Membr. Sci.* **2009**, *327*, 78.

84 F. Liu, C.-H. Du, B.-K. Zhu, Y.-Y. Xu, *Polymer* **2007**, *48*, 2910.

85 Y. Chang, C.-Y. Ko, Y.-J. Shih, D. Quémener, A. Deratani, T.-C. Wei, D.-M. Wang, J.-Y. Lai, *J. Membr. Sci.* **2009**, *345*, 160.

86 P. Kanagaraj, A. Nagendran, D. Rana, T. Matsuura, S. Neelakandan, R. Revathi, N. Pandiyarajan, *Polym. Eng. Sci.* **2015**, *55*, 2482.

87 Q. Li, Z.-L. Xu, L.-Y. Yu, *J. Appl. Polym. Sci.* **2010**, *115*, 2277.